



ELSEVIER

Contents lists available at ScienceDirect

## Global and Planetary Change

journal homepage: [www.elsevier.com/locate/gloplacha](http://www.elsevier.com/locate/gloplacha)

# On the relationship between north India summer monsoon rainfall and east equatorial Indian Ocean warming

Ramesh Kumar Yadav<sup>a,b,\*</sup>, Mathew Koll Roxy<sup>b,c</sup>

<sup>a</sup> Plants, Soils and Climate Department and Utah Climate Center, Utah State University, Logan, Utah, USA

<sup>b</sup> Indian Institute of Tropical Meteorology, Pashan, Pune, India

<sup>c</sup> NOAA/Pacific Marine Environmental Laboratory, Seattle, Washington, USA

## ARTICLE INFO

## Key words:

Indian summer monsoon

North India

Deep convection: sea surface temperature

Equatorial Indian Ocean

Tibetan Plateau

Rossby wave gyres

## ABSTRACT

Generally, a strong north India summer-monsoon rainfall (NISR) is associated with anomalous upper troposphere ridge over northwest of India. This ridge triggers anomalous northerly winds over Tibetan Plateau and easterlies over India. The easterly anomaly over India reduces the tropospheric wind shear, while the northerly at Tibetan plateau allows frequent intrusions of high-latitude dry and cold meridional winds to interact with the lower-level relatively warm and moist easterly monsoonal flow, enhancing the NISR. The current study, using a suite of observations, reanalysis products and numerical model sensitivity experiments, explores the changes in NISR, and its association with the warming in the equatorial Indian Ocean.

In the recent two decades (1996–2017), the NISR has been exhibiting a decreasing trend with increased variability, much larger than the earlier period (1979–2000). A possible reason for this is due to the rise in warm sea surface temperature (SST) observed in the east equatorial Indian ocean, which shows a negative correlation to NISR. The current analysis indicates that the warmer SST induce strong convection and associated northward propagating off-equatorial Rossby gyres to the west of the equatorial eastern Indian ocean, spreading the tropospheric heating towards the northeast of India, thereby elevating the geopotential height. This creates upper troposphere low pressure anomaly at the northwest of India. These factors are consistent with the suppression of the NISR, resulting in the observed decreasing trend in the recent decades.

## 1. Introduction

The South Asian monsoon, especially that over the Indian subcontinent can be considered as one of the strongest and the most significant phenomenon in the tropical climate. Agriculture and the entire ecosystem of the Indian subcontinent depend upon this monsoonal rain, which occurs during June to September (JJAS), also known as Indian summer monsoon (ISM). The northern part of India consists of one of the richest fertile land of the Gangetic Plain and the world's largest population density. North India is home to more than 7 percent of the world's population. The main occupation in this region is agriculture and husbandry, which heavily depends on the variability of the north India summer-monsoon rainfall (NISR). Therefore, the spatial and temporal variations of NISR, manifested in the floods and droughts, have a significant impact on agricultural yields and livelihood of the people living in this region.

The north Indian region, in the proximity of the foot hills of Himalayas, gets heavy rainfall during the summer season (JJAS). The

rainfall over north India extending to the foot hills of Himalayas are supposed to be enhanced when the monsoon is in a break phase over central India. During this phase, the monsoon trough shifts northwards from its normal position towards the foothills of Himalayas, while central India is marked by anomalous high pressure. At the upper-level, the large amplitude westerly trough intrudes into the northern parts of India and give rise to heavy rainfall (Ramamurthy, 1969; Krishnamurti and Ardanuy, 1980; Ramaswamy, 1956, 1962; Raman and Rao, 1981). And, also the interaction between the strong monsoonal flows and the high amplitude westerly trough embedded in the westerly jet (Vellore et al., 2014) produces heavy rainfall over north India.

The inter-annual variability of Indian rainfall is strongly influenced by the El-Niño-Southern Oscillation (ENSO) (Kumar et al., 1999; Ashok et al., 2004; Yadav, 2009a, 2009b), the Indian Ocean Dipole Mode (Saji et al., 1999; Webster et al., 1999; Ashok et al., 2004; Crétat et al., 2017), the tropical Atlantic/Atlantic Niño (Goswami et al., 2006; Kucharski et al., 2008; Yadav, 2017a; Yadav et al., 2018) and the surface temperature/pressure over the Middle-East (Yadav, 2016, 2017b).

\* Corresponding author at: Indian Institute of Tropical Meteorology, Pashan, Pune 411008, India.

E-mail address: [yadav@tropmet.res.in](mailto:yadav@tropmet.res.in) (R.K. Yadav).

<https://doi.org/10.1016/j.gloplacha.2019.05.001>

Received 14 November 2018; Received in revised form 3 April 2019; Accepted 1 May 2019

Available online 02 May 2019

0921-8181/ © 2019 Elsevier B.V. All rights reserved.

The summer monsoon rainfall over the central and northern parts of India has been showing a decreasing trend since the 1950s, according to several studies (Annamalai et al., 2013; Ratna et al., 2016; Ramanathan et al., 2005; Roxy et al., 2015). Ramanathan et al. (2005) attribute the drying trend to a change in meridional temperature gradients, due to increased aerosols concentrations. Meanwhile, Annamalai et al. (2013) argue that the SST warming over the tropical west Pacific causes a drying trend over South Asia due to changes in the atmospheric circulation, by which drier, cooler air is advected from northeast India towards Bay-of-Bengal and the Indian subcontinent. Ratna et al. (2016) suggests a weakening of the low-level monsoon westerlies in association with the Indo-Pacific warming should modulate the local Walker circulation. Several studies (Roxy et al., 2015; Krishnan et al., 2016; Paul et al., 2016) point out that the decline in the mean rainfall over central India is consistent with a dampening of the local Hadley circulation, due to a combination of factors including the rapid warming of the Indian Ocean, land use-land cover changes, and increased aerosol content in the atmosphere. Qu and Huang (2012) documented that the tropical Indian Ocean warming since the 1970s has significantly distributed the tropospheric warming over the global tropics. To the east of the equatorial Indian Ocean, the warm anomaly displays a Kelvin wave-like response and to the west a Rossby wave-like pattern, with two maximums off the equator. The Kelvin and Rossby wave-like patterns display the Matsuno–Gill (Matsuno, 1966; Gill, 1980) pattern, indicating they are the responses to the Indian Ocean heating. This tropospheric response is apparent in the anomalous increase in upper-tropospheric geopotential height. A recent study by Jin and Wang (2017) have shown a revival of ISM after 2002 due to the warming of the Indian continent and slower rate of warming of the Indian Ocean. However, the high resolution rainfall data from the Indian Meteorological Department (IMD) exhibits decreasing trend in the plains of north India even during this period.

The monsoon rainfall over the plains of north India is comparatively less studied with respect to central India. The main objective of this study is to understand the dynamics and the teleconnections of the seasonal summer monsoon rainfall over the plains of north India and the possible reason for the decreasing trend in rainfall during the recent decades, when the rainfall over other regions of India is showing a revival since early 2000. The north India monsoon circulation pattern is poorly understood. In this study, we propose a hypothesis that the decreasing trend in NISR is due to increased SSTs over the eastern equatorial Indian Ocean. This has raised the tropospheric height towards the northeast India, creating low pressure anomalies over northwest India and east Asia with anomalous northerly wind over the Tibetan Plateau. These are unfavorable for NISR. The results of the study are corroborated using numerical model sensitivity experiments.

## 2. Data and methods

The reanalysis products from the European Centre for Medium-Range Weather Forecasts *ERA-Interim* dataset available at a  $0.75^\circ$  spatial resolution (Dee et al., 2011) is used for the period 1979–2017. It has been noted that the trends observed in the long-term reanalysis data are subjected to artificial shifts due to the introduction of widespread satellite data in the late-seventies (Kinter et al., 2004). Neither data availability nor long-term consistency in data quality is sufficient for detecting and examining this long-term climate trends and/or multi-decadal climate variability (Trenberth et al., 2008). Therefore, the *ERA-Interim* dataset available after late-seventies—that is, from 1979 till date, is most reliable and realistic. The observed monthly gridded rainfall data over the Indian landmass used in this study is from the Indian Meteorological Department at a resolution of  $0.25^\circ \times 0.25^\circ$  for the period 1979–2017 (Pai et al., 2014). The daily Outgoing Longwave Radiation (OLR) dataset (Liebmann and Smith, 1996) is used to plot the Wheeler-Kiladis Space-Time Spectra (Hendon and Wheeler, 2008) and time-latitude plot to show the equatorially trapped planetary waves

(Kelvin and Rossby) and northward propagation of Rossby waves.

The methods used are simultaneous correlation and regression on the detrended dataset. The excess and deficient years are considered  $\pm 1$ SD of the long-term mean. For the climate model sensitivity experiments, we use the standard configuration of the Climate Forecast System version 2 (CFSv2), a global coupled ocean-atmosphere model. The CFSv2 model simulates the ENSO and the mean monsoon reasonably well and hence used in this study (Roxy et al., 2013). The oceanic component is the GFDL MOM4, at a  $0.25\text{--}0.5^\circ$  horizontal resolution, with 40 vertical levels and an interactive ice model. The atmospheric component is the NCEP GFS, which adopts a spectral triangular truncation of 126 waves (T126) in the horizontal ( $\sim 0.9^\circ$ ) and a finite differencing in the vertical with 64 sigma-pressure hybrid layers. The atmosphere and ocean model components exchange the heat and momentum fluxes every half an hour, with no flux adjustment or correction. The coupled configuration of CFSv2 is time integrated over a period of 40 years, and utilized as the reference run (CFSv2<sub>CTL</sub>). Ensembles (10 members) of short integrations for the summer monsoon season during June–September were performed by adding temperature anomalies to the SSTs passed over the equatorial Indian Ocean, to the atmosphere (CFSv2<sub>EQIO</sub>). Positive anomalies of the order of  $1.0^\circ\text{C}$  was added over the region, in such a way that it tapers out by the limits of the domain ( $55^\circ\text{E}\text{--}95^\circ\text{E}$ ,  $5^\circ\text{S}\text{--}5^\circ\text{N}$ ). The difference between CFSv2<sub>EQIO</sub> and CFSv2<sub>CTL</sub> is taken as the model response to the summer warming over the equatorial Indian Ocean.

## 3. Results

### 3.1. JJAS India rainfall trend and atmospheric dynamics

A study by Jin and Wang (2017) documented the revival of Indian summer monsoon since 2002, but the trend analysis of the seasonal JJAS India rainfall for the period 1979–2017 (Fig. 1a) shows a big patch of the drying trend over the plains of north India. This is consistent with other studies (Ramanathan et al., 2005; Annamalai et al., 2013; Roxy et al., 2015). It is hence intriguing to know why the revival of monsoon is not observed in the plains of north India. The region under consideration consists of Bihar and Uttar Pradesh, two highly populated states of India where livelihood is solely dependent on rain-fed agriculture. The summer monsoon rainfall in this region is comparatively very less studied and poorly understood. However, it is thought that the main component of the rain in this region is the northward movement of the monsoon trough from its normal position and the interaction between the westerly trough and the monsoonal flow (Ramamurthy, 1969; Krishnamurti and Ardanuy, 1980; Ramaswamy, 1956, 1962; Raman and Rao, 1981; Vellore et al., 2014). Further, to examine the possible reason and cause of this decreasing trend in rainfall over north India and its teleconnections, the time-series has been prepared by averaging the gridded rainfall over the box ( $78.5^\circ\text{E}\text{--}87.5^\circ\text{E}$ ,  $24^\circ\text{N}\text{--}28.5^\circ\text{N}$ ), named hereafter as NISR. A correlation analysis between NISR and India rainfall shows significant positive correlation coefficients (CC) over most parts of north India (Fig. 1b), but not over other regions. This suggests that the NISR is largely independent of the monsoon rainfall variability over central India or northeast India. The fact that the revival of central Indian monsoon rainfall in the recent decade is not observed in this region illustrates this point. Therefore, this should be studied separately to avoid the results getting obscured due to the rainfall processes over central India and northeast India. Studies in the past have frequently included this region along with the central India or northeast India monsoon domain, which can be misleading. The standard deviation pattern (Fig. 1c) shows 2.4–3.3 mm/day, suggesting a high variability in this region during summer season JJAS.

Fig. 2 shows the regression of 250-, 500- and 850-hPa winds onto NISR (red arrows) and the CC of NISR versus 250-hPa GPH (contours, Fig. 2a) and SST (shaded, Fig. 2e) in the left panels superposed with

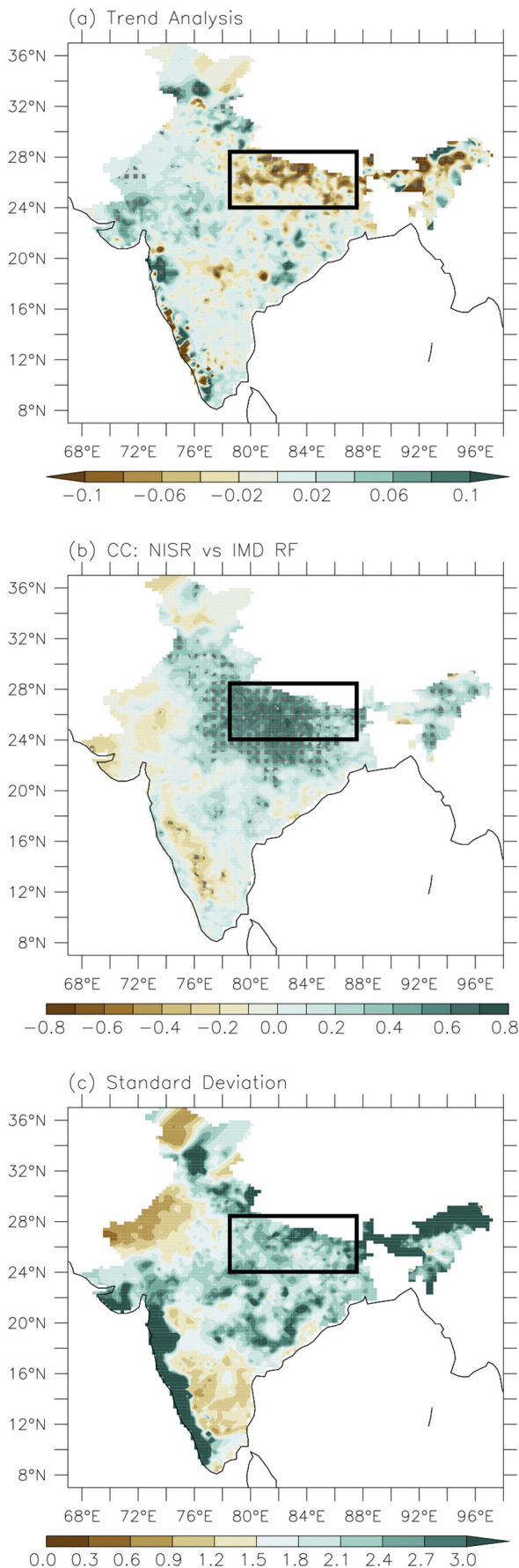


**Fig. 1.** IMD data analysis: (a) JJAS seasonal trend analysis for India rainfall. Areas of 95% significance level are shaded by tiny grey dots. (b) Simultaneous correlation coefficients between NISR and IMD RF data. Areas of 95% significance level are shaded by tiny grey dots. (c) Standard Deviation of India rainfall (mm/day) for the period 1979-2017. The box represents the NISR region.

geographical height over the land. The right panels show 250-, 500- and 850-hPa vertical velocity (shaded) and vorticity (contours). The SST pattern (Fig. 2e) shows significant negative CC over the eastern equatorial Indian Ocean. The eastern equatorial Indian Ocean SST is important as the atmospheric response is largely dependent on the mean SSTs, which are cooler in the western Indian Ocean and warmer in the east. As a result, the response in convection and hence the atmospheric circulation is enhanced even due to slight changes in the eastern equatorial Indian Ocean SSTs. The 850-hPa wind anomaly shows the stronger southwesterlies over Arabian Sea and cyclonic convergence over central/central-east India associated with easterly anomaly over the NISR region. The 850-hPa vorticity (Fig. 2f) shows the strong positive vorticity CC over north India and strong negative vorticity CC along the foot hills of Himalaya towards the northeast NISR region. The strong negative vorticity anomaly in the proximity of foot hills of Himalayan region is due to reflection of winds from the mountains causing divergence. The anomalous wind represents the climatological patterns, revealing strong monsoon trough accompanied with the intense moisture laden easterly monsoonal flow over the NISR region at the lower-level. The negative vertical velocity anomaly at NISR region indicates strong convection. At 500-hPa level (Fig. 2c&d), the significant easterly wind, vorticity and vertical velocity anomalies over NISR region persist. The CC of 250-hPa GPH (Fig. 2a, contours) shows significant positive CC northwest of India. The winds anomaly (Fig. 2a) shows significant easterly over India and Arabian Sea, and northerly over Tibetan Plateau. The positive GPH anomaly over northwest of India produce anomalous easterly over India and northerly over Tibetan Plateau. Meanwhile, the anti-cyclonic circulation anomaly north of India results in negative vorticity CC north of NISR region (Fig. 2b). Further, the anomalous upper troposphere northerly along the Tibetan Plateau suggests the mid-latitude interaction of dry and cold air with the lower level warm and moisture laden strong monsoonal flow, which incites deep convection and enhanced rainfall over NISR region. In addition, the anomalous winds are easterly from the lower to the upper troposphere over the NISR region, weakening/minimizing the tropospheric wind shear, favorable for deep convection. Over NISR region, the weaker tropospheric wind shear promotes strong convection, while the strong tropospheric wind shear kills the strong convection.

To study the interaction between the lower-level monsoonal flow and the upper-troposphere meridional wind, we have selected two boxes 1) zonal wind over 79.5°E-87.5°E, 25.5°N-28.5°N at the 850-hPa, representing the lower-level monsoonal flow, and 2) meridional wind over 84.75°E-97.5°E, 26.25°N-39.75°N at the 250-hPa, representing the upper-troposphere mid-latitude penetration into north India. The CC of NISR with these lower-level zonal wind index and upper-troposphere meridional wind index are -0.48 and -0.33, significant at 99% and 95% confidence levels. Moreover, the CC between the upper and lower troposphere index is 0.43, statistically significant at 99% confidence level, suggesting the strong association among them and with NISR.

### 3.2. Time-series trend analyses

The NISR time series shows a significant decreasing trend of  $-0.03865$  mm/day for the entire study period during 1979-2017, significant at 98% confidence level (Fig. 3a). The decreasing trend is much larger in the last two decades, from 1996-2017 ( $-0.0443$ , period 2), than the earlier period 1979-2000 ( $-0.02485$ , period 1). The mean has decreased (from 7.667mm/day to 6.986mm/day), but the



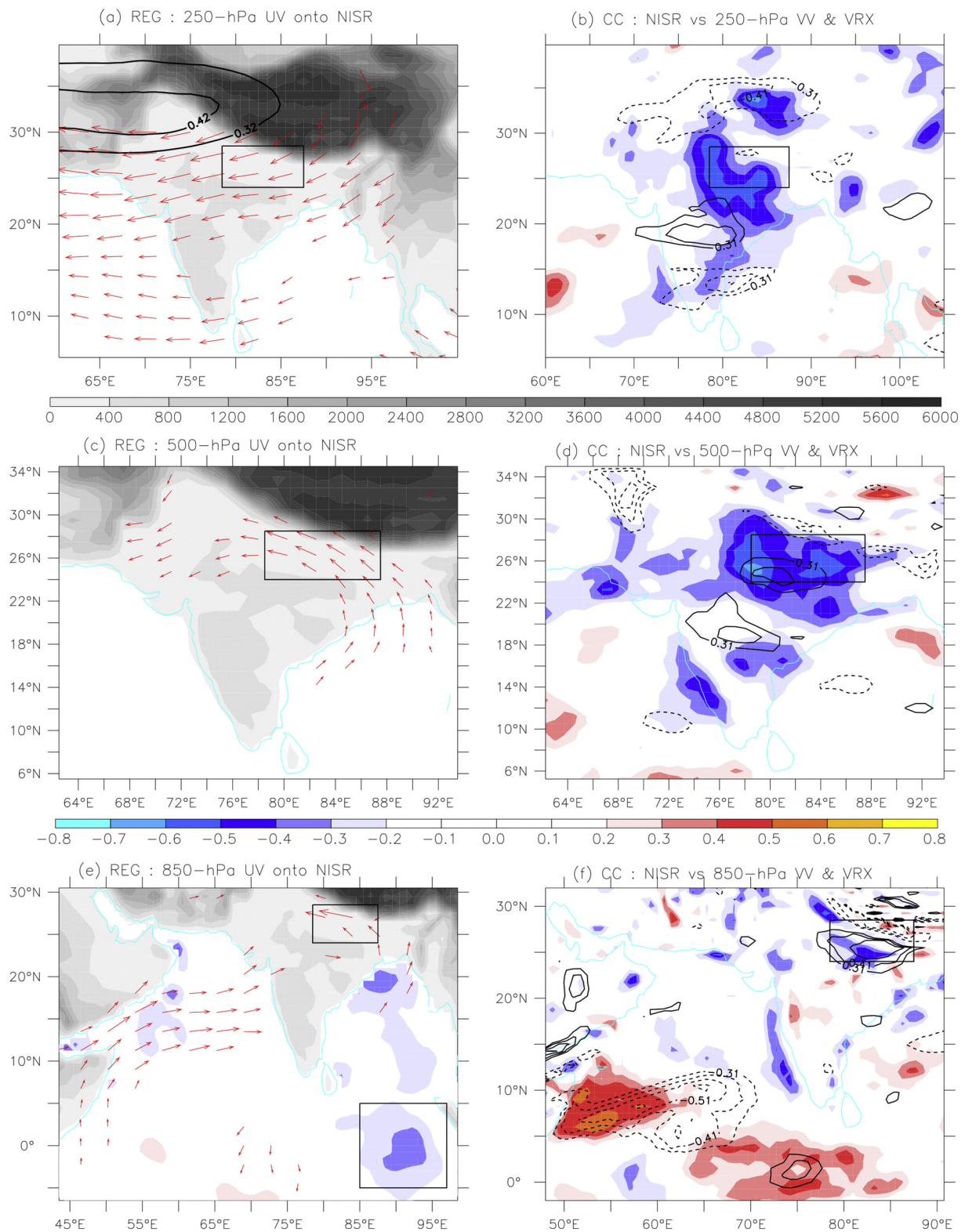


**Fig. 2.** Regression of (a) 250-, (c) 500- and (e) 850-hPa wind onto NISR. The grey shading is the altitude. Correlation coefficients of NISR with (a) 250-hPa GPH (contours), (e) SST (color shade), (b) 250-, (d) 500- and (f) 850-hPa vertical velocity (color shade) and vorticity (black contours). (For interpretation of the references to color in this figure legend, the reader is referred to the web version of this article.)

variability has increased (standard deviation from 0.9686mm/day to 1.1733mm/day) in the period 2, as compared to the period 1. This clearly shows the distinction between the two epochs in the NISR, consistent with the recent study (Ratna et al., 2016). Recently, Jin and Wang (2017) reported a short-term increase in the Indian summer

monsoon since 2002. This revival is associated with the warming of the Indian continent and slower rates of warming of the Indian Ocean during 2002–2014. Besides, extended SST data until the year 2017 shows significant warming in the Indian Ocean SSTs (Roxy, 2017). However, the north India summer rainfall has not revived, but the

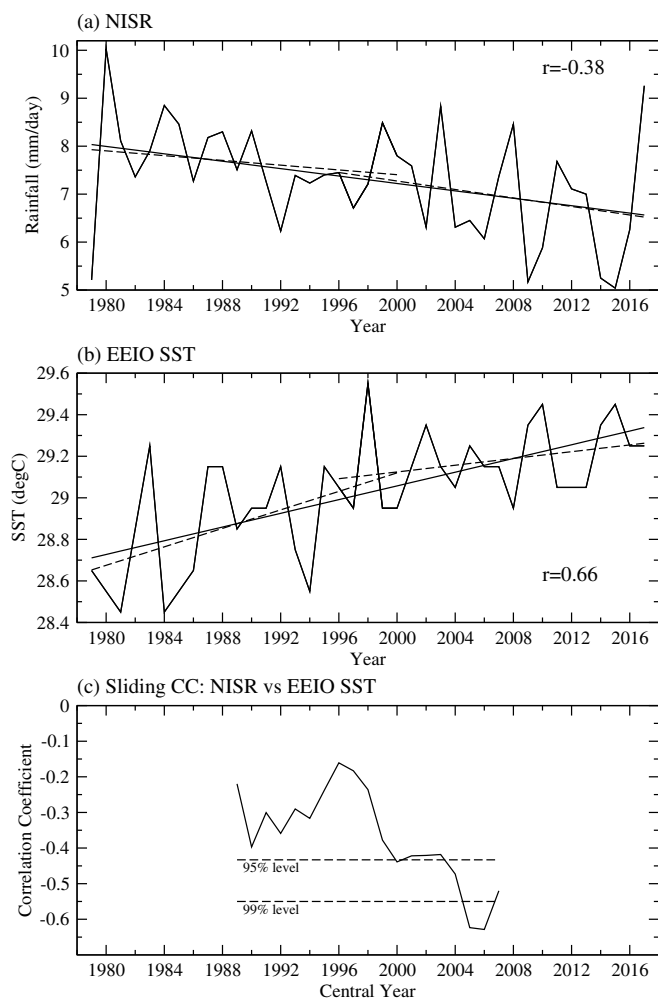


**Fig. 3.** Time-series of (a) NISR (mm/day), (b) EEIOSST and (c) sliding CC on a 21-year moving window between EEIOSST and NISR. The straight black line in a and b represents the trend line for the entire period and the straight dashed line represents the trend line for the respective epochs. The black dash line in c represents the 95% and 99% significance levels.

drying trend has further steepened with increased variability.

The eastern equatorial Indian Ocean SST (EEIOSST) which shows the significant negative CC over the box (85°E–97°E; 5°S–5°N) has been averaged to study its relationship to NISR. The EEIOSST (Fig. 3b) shows a significant increasing trend of 0.0165°C/month throughout the data period, significant at 99.9% level, consistent with other studies (Roxy et al., 2015; Ratna et al., 2016; Abish et al., 2018; Annamalai et al., 2013). The trend is larger in the period 1 in comparison with the period 2. In the period 2, EEIOSST shows a slower rate of warming, but the SST values are always greater than 28.94°C.

The 21-year sliding CC with NISR (Fig. 3c) shows the secular relationship between NISR and EEIOSST. The relationship shows shift around late-1970s, the CC became significant, with the CC reaching the 98% confidence level in the last two decades. It is noted that the convection increases with increasing SST, and the rate of increase of convection can be very large for the SST range of 27°–28°C (Lau et al., 1997). Thus, despite a slower rate of warming in the period 2, the SST anomalies are sufficient enough to anchor the in-situ vigorous convection. In all the deficient years, when the NISR was less than 200mm, the EEIOSST was greater than 29°C, such as 1992, 2002, 2004, 2005, 2009, 2010, 2014 and 2015. In contrary, the flood years, with NISR more than 270mm, the EEIOSST are less than 28.6°C, such as 1980 and 1984. These results confirm a possible relationship between the

EEIOSST and NISR.

### 3.3. Significant difference between period 1 and period 2

To study the significant difference in the mean of the two epochs: period 1 and period 2, student's *t*-test analysis has been done on the SST, 250-hPa GPH, 850- and 250-hPa wind, and shown in Fig. 4. The SST (Fig. 4a) shows significant difference over the equatorial Indian Ocean, consistent with studies (Roxy et al., 2015; Ratna et al., 2016; Abish et al., 2018; Annamalai et al., 2013). However, the atmospheric response is largely dependent on the mean SSTs, which are cooler in the western Indian Ocean and warmer in the east. As a result, the response in convection and hence the atmospheric circulation is enhanced over the eastern equatorial Indian Ocean, where the north Indian summer monsoon rainfall is significantly correlated. It is argued that the warming in the east equatorial Indian Ocean SST is related to the natural variability of the Indian Ocean, rather than the influence from the Pacific (Abish et al., 2018). The 850-hPa wind shows strong cross-equatorial monsoonal flow over western Arabian Sea and south Indian Ocean, consistent with the study (Ratna et al., 2016). The winds are not significant over India or NISR region. The 250-hPa GPH (Fig. 4b) shows significant increase of GPH over northeast of India associated with anti-cyclonic circulation with southerly wind component over Tibetan Plateau. The rise in anomalous southerly wind component over the Tibetan Plateau in the period 2 hinders the mid-latitude/extra-tropical interaction with the lower level monsoonal flow, which has resulted in enhancing the decreasing trend and increasing the variability of the NISR compared to period 1. Meanwhile, the lower-level monsoonal flow towards the NISR region has not changed significantly. This indicates that the upper-troposphere southerly wind anomalies over the Tibetan Plateau, associated with the negative and positive GPH anomalies over northwest and northeast of India, are responsible for the enhanced decreasing trend in NISR.

### 3.4. East equatorial India Ocean SST

In order to investigate the influence of EEIOSST on the upper-tropospheric circulation features during period 1 and period 2, we conducted separate correlation analysis between EEIOSST and vertically integrated tropospheric temperature from 650- to 175-hPa, 250-hPa GPH and a regression analysis of 250-hPa winds onto EEIOSST for these two periods (Fig. 4c,d,e&f). The vertically integrated tropospheric temperature is chosen between 650- to 175-hPa as the monsoonal latent heating is evident between these levels. Fig. 4c&d shows that the EEIOSST warming significantly warms the tropical troposphere. To the east of the EEIO, the narrow warm anomaly along the equator displays a Kelvin wave response and to the west the widespread warm anomaly along the tropics represents a Rossby wave pattern. Similar type tropospheric temperature warming pattern by the equatorial Indian Ocean SST has been shown by Qu and Huang (2012), (Fig. 4b). These Kelvin and Rossby wave patterns display the Matsuno-Gill pattern (Matsuno, 1966; Gill, 1980). This indicates that the EEIOSST affects the tropospheric temperature through enhanced convection and moist adjustment. These convectively coupled equatorial Rossby and Kelvin waves are the most important in the tropics as they modulate a wide range of weather and climate phenomenon, such as ENSO, monsoons, tropical cyclonic circulation and mid-latitude weather. The Rossby wave exhibit pairs of cyclonic and anticyclonic gyres straddling the equator, which propagates poleward and westward. The Rossby wave displays maximum variability in the northern hemisphere during boreal summer (Huang and Huang, 2011). In the period 2, when the EEIOSST is much warmer than the period 1, the CCs are much stronger. Also, the poleward extension of anomalous tropospheric warming towards northeast India is much deeper and widespread in the period 2 compared to period 1. This suggests that the stronger convection in the period 2 due to the stronger warming of EEIOSST has generated stronger Rossby and

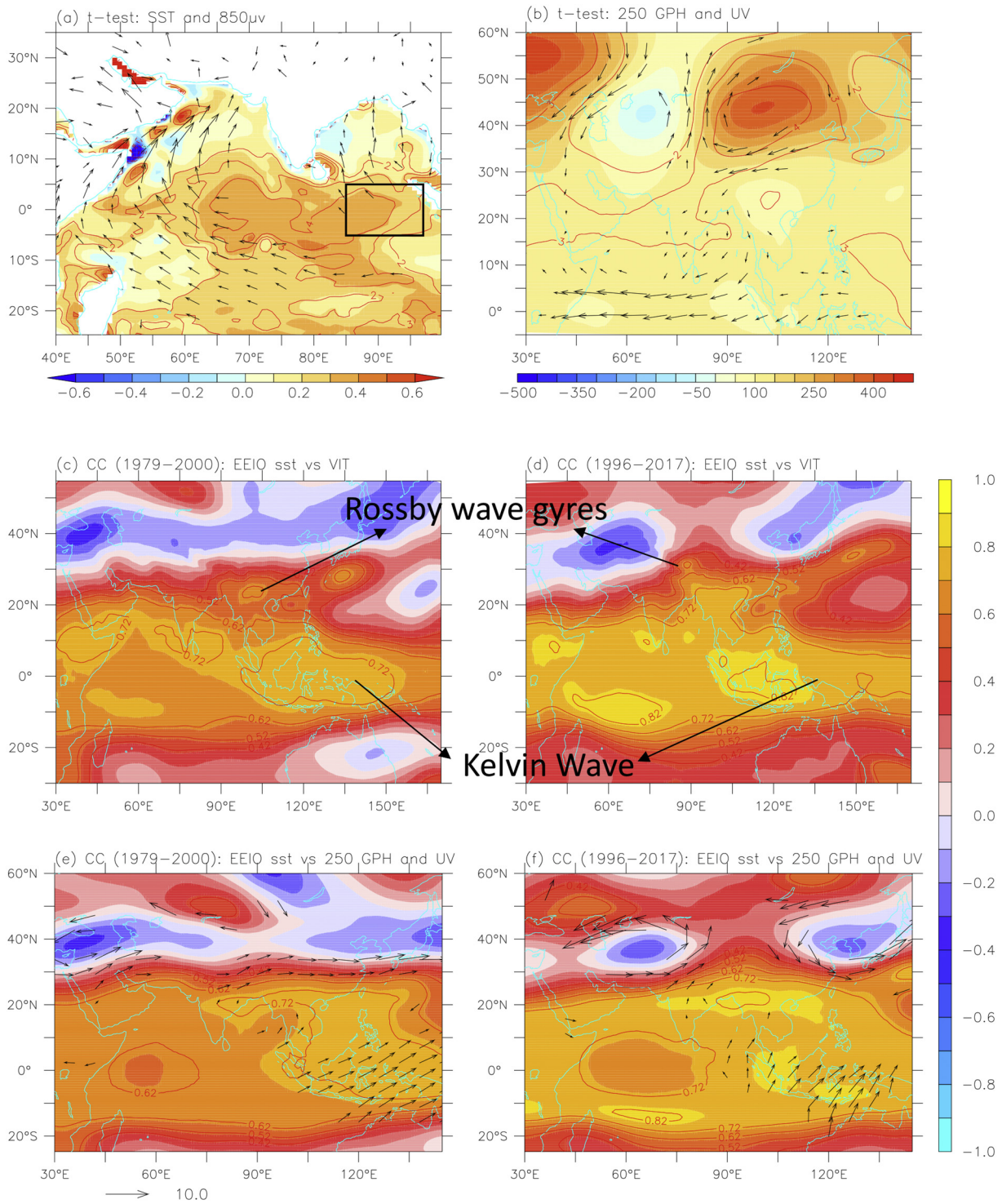


**Fig. 4.** Student t-test in the mean of the two epochs: 1979-2000 (period 1) and 1996-2017 (period 2) for (a) SST and 850-hPa winds, and (b) 250-hPa GPH and winds. Red contours are significant at 95% level. Simultaneous correlation coefficients of EEIOSST with (c) vertically integrated temperature from 650- and 175-hPa for (c) period 1 and (d) period 2 and 250-hPa GPH and regression of 250-hPa wind onto EEIOSST (e) period 1 and (f) period 2.

Kelvin waves compared to period 1. The off-equatorial Rossby wave gyres were displaced more poleward, spreading the tropospheric warming more towards the northeast of India in the period 2.

Fig. 4e,f CC patterns indicates an elevation of troposphere height over the tropical Indian Ocean, with the maximum anomaly over Bay of Bengal and the warm-pool region of Indonesia due to the intensification of convection over the anomalously warm EEIO. The notable differences are: the negative GPH CC is zonally elongated between 30°N-40°N

from Middle-East to east Asia associated with anomalous zonal winds towards the southern fringe of negative GPH CC between 20°N-35°N in the period 1, while in the period 2 the significant positive GPH CC has penetrated up to northeast of India forming two negative pressure anomalies over northwest of India and east Asia accompanied with anomalous southerly winds over the Tibetan Plateau. The maximum poleward displacement of off-equatorial Rossby wave gyres towards the northeast of India during period 2 has raised the tropospheric height



extending to northeast of India. This clearly displays the notable increase in upper-troposphere GPH towards the northeast of India during period 2 (compared to the period 1, Fig. 4d) due to the warmer EEIOSST during this period (Fig. 3b). It is to be noted that during the period 1 the warm EEIOSST has imposed anomalous westerly over north India. Moreover, in the period 2 the warm EEIOSST has imposed anomalous southerly over the Tibetan Plateau and westerly over north India both, enhancing the decreasing trend and increasing variability of the NISR.

The simultaneous CC between NISR and EEIOSST for the two periods—that is, period 1 and period 2 are  $-0.144$  and  $-0.49$ , respectively. For period 1 the CC is not significant, while for period 2 the CC is significant at 98% confidence level. For the entire period—that is, 1979–2017, the CC is  $-0.274$  significant at 90% confidence level. This indicates that in period 1 when the EEIOSST was below  $28.6^{\circ}\text{C}$  the influence of EEIOSST was overlooked, but in period 2 when the EEIOSST increased above  $28.6^{\circ}\text{C}$  the in-situ vigorous convection and moist adjustment owing to the SST anomalies affect largely the tropospheric temperature. This affected the upper-tropospheric pressure and related wind and thus the NISR.

Further, we have plotted wavenumber-frequency power spectrum (Hendon and Wheeler, 2008) for the daily OLR data for JJAS at each latitude and averaged from  $15^{\circ}\text{N}$  to  $15^{\circ}\text{S}$  (Fig. 5a&b) to extract the equatorially trapped planetary waves: eastward propagating Kelvin and westward propagating Rossby waves. To highlight this, we chose two contrasting years, during which SSTs in the east equatorial Indian ocean were high (1992, SST greater than  $29^{\circ}\text{C}$ ) and low (1980, SST less than  $28.6^{\circ}\text{C}$ ), and were non-ENSO years. Both the years shows equatorially trapped eastward and westward propagating Kelvin and Rossby waves, respectively. Now to assess the off-equatorial poleward movement of the Rossby wave west of the warmer eastern equatorial Indian Ocean, we have plotted the time-latitude daily OLR anomaly (averaged over the longitudes  $70\text{--}77.5^{\circ}\text{E}$ ) for June–September (Fig. 5c&d). The year 1992 clearly shows more frequent and stronger northward propagation of the cyclonic and anticyclonic Rossby wave gyres. Meanwhile 1980 shows infrequent and weaker northward propagation of Rossby wave gyres compared to the year 1992. Although equatorial Rossby wave can occur at any longitude, the background thermal-dynamics conditions such as warmer SST and larger moisture content favors deep convection and thus the Rossby waves (Huang and Huang, 2011). Therefore, the equatorial warming of eastern equatorial Indian Ocean SST produces stronger northward propagating Rossby waves gyres towards north India in the year 1992 compared to 1980.

### 3.5. Model results

In order to confirm the monsoon response to the summer warming over the east equatorial Indian Ocean, coupled model experiments were conducted with SST anomalies (equivalent to the observed trends) imposed over the east equatorial Indian Ocean (Fig. 6a). See Saha et al. (2013) for further details on the model and its components, and Roxy et al. (2015) for a similar numerical experiment setup. The model sensitivity experiments indicate that the warm east equatorial Indian Ocean is associated with strong convection which generates off equatorial Rossby gyres to the west of the convection which spreads up to northeast of India heating the troposphere and elevating GPH (Fig. 6b). In addition, in the deep tropics, horizontal variations of GPH are much smaller, since it is difficult to maintain them in the presence of the weak Coriolis force, while in the mid-latitude/extra-tropics the GPH variations are much higher due to the presence of higher Coriolis force. Therefore, in the tropical regions of Indo-Pacific Ocean the GPH positive anomaly is much smaller, while over mid-latitude the anomaly is much bigger respectively. The elevation of GPH over northeast of India has separated two low pressure anomalies over northwest of Indian and east Asia, associated with southerly wind over Tibetan Plateau, consistent with the observation (Fig. 4b). This southerly wind hinders the

interaction of upper-troposphere dry winds from mid-latitude/extra-tropical winds to the lower-level monsoonal wind and hence decreasing NISR. The two low pressure areas over northwest of India and east Asia and high pressure area over northeast of India with southerly winds over Tibetan Plateau due to east equatorial Indian Ocean warming, is very well captured by the model and is in agreement with the observation.

## 4. Discussion

The current study focuses on the recent decreasing trend in rainfall during the summer monsoon season (June–September) in north India for the period 1979–2017, when the monsoon has revived in the most part of India since early 2000. Since the Indian monsoon exhibits variability on decadal timescales, and since the analysis period is not long enough to conclude on long-term trends, it is difficult to establish if these observed changes in rainfall are part of natural variability or anthropogenic changes in the climate. Nevertheless, we try to explore the underlying mechanisms dominating the observed changes in the north Indian summer rainfall (NISR). The analysis shows that the NISR manifest as the combined contribution of the interaction between the lower-level moisture laden monsoonal flow and the upper-tropospheric dry and cold meridional winds. The low-level monsoonal flow is comparatively warm and moist, and therefore lighter than the upper-tropospheric cold dry air from the mid-latitudes. When these northerly winds from the Tibetan Plateau interact with the monsoonal flow, they uplift the warm and moist monsoonal air as they are lighter than the northerly winds coming from east Asia. Generally, this triggers the deep convection over north India. Also, the Himalayas in the north play the role to steer the winds cyclonic at the lower level, conducive for the convection to occur.

The upper-troposphere meridional wind over the Tibetan Plateau and equatorial Indian Ocean shows substantial difference between the two epochs i.e. first 22-years (1979–2000) and last 22-years (1996–2017). The significant changes in the mean in these parameters show warm SST over the equatorial Indian Ocean, decrease in northerly over the Tibetan Plateau, and decreased rainfall in the later period over NISR. On the other hand, a study by Jin and Wang (2017) reported that a strong warming of the Indian subcontinent accompanied by a slower rate of warming over the Indian Ocean has revived the monsoon over central India since early 2000, due to a strengthening of the land-ocean temperature gradient. The present study reveals that the warming of the eastern equatorial Indian Ocean promotes increased tropospheric moisture to anchor the in-situ convection, generating off equatorial Rossby gyres to the west. This spread tropospheric heating towards the northeast of India, elevating geopotential height (GPH) in the recent decades. The elevated GPH has separated two low pressure anomalies over northwest of Indian and east Asia, associated with anomalous southerly wind over the Tibetan Plateau. This southerly wind hinders the interaction of upper-troposphere dry winds from mid-latitude/extra-tropical winds to the lower-level monsoonal wind, thereby reducing the NISR. However, the changes in Indian Ocean alone may not be responsible for the observed changes in monsoon rainfall. Changes in land cover from trees to crops and changes in land use in the recent decades may also have contributed to the observed weakening of the monsoon, by reducing the evapotranspiration and thereby the recycled component of rainfall (Paul et al., 2016). Also, differential heating in the basins can induce changes in moisture transport, which may also get reflected in the monsoon rainfall over north India (Vishnu et al., 2016). Therefore, land surface processes are important for understanding the changes in monsoon over central and north India. In the present study, we focus only on the effect of ocean warming on the monsoon rainfall, which is significantly large and has a major impact on the monsoon.

Earlier studies suggest that the summer monsoon rainfall is active over north India while the rainfall is subdued over central India, due to a northward shift of the monsoon trough (Ramamurthy, 1969;

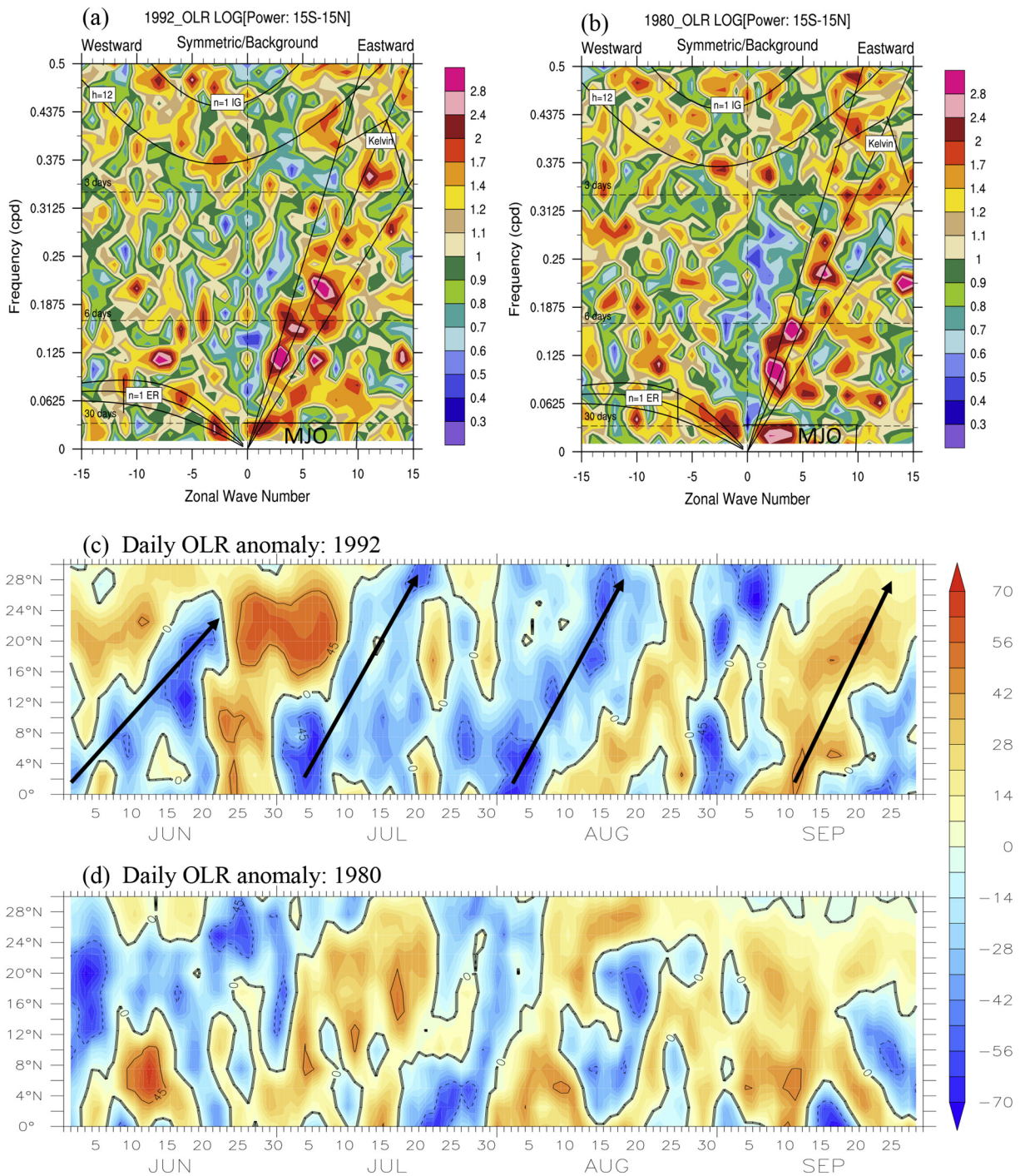


**Fig. 5.** Frequency-wavenumber spectra for the daily OLR data during JJAS for the two extreme years (a) 1992 and (b) 1980. The time-latitude daily OLR anomaly plot (averaged over the longitudes 70–77.5°E) for JJAS for the year (c) 1992 and (d) 1980. The black arrows in (c) shows the northward movement of Rossby wave gyres.

Krishnamurti and Ardanuy, 1980; Ramaswamy, 1956, 1962; Raman and Rao, 1981). Recent studies (Annamalai et al., 2013; Ratna et al., 2016) argued that the drying of NISR is due to changes in the lower-level circulation. The current study, for the first time, shows that the drying of NISR is due to increase of anomalous upper-troposphere southerly winds over Tibetan Plateau owing to the warm equatorial Indian Ocean in the recent two decades. The north India rainfall is enhanced when the monsoon flow is strong, and the central India rainfall is normal. The strong monsoonal flow gets reflected by the foot hills of Himalayas and produces the cyclonic vortices at the lower level. At the middle to upper tropospheric level the weaker westerly reduces

the tropospheric wind shear conducive for the deep convection and allows the frequent interaction of northerly wind from the Tibetan Plateau with the lower-level monsoonal flow, that results in copious rainfall in the region. Though Indian rainfall is available for long-term, high quality ocean-atmospheric data is not available before satellite-era, which is why we are restricting this study to post-1979, during which reliable and realistic reanalysis data are available. Considering the rapid and intense warming in the Indian Ocean (Roxy et al., 2014), and given the fact that CMIP5 models project further warming in the Indian Ocean, it is imperative that we pay attention to the remote links and mechanisms explored in this study for improved understanding and



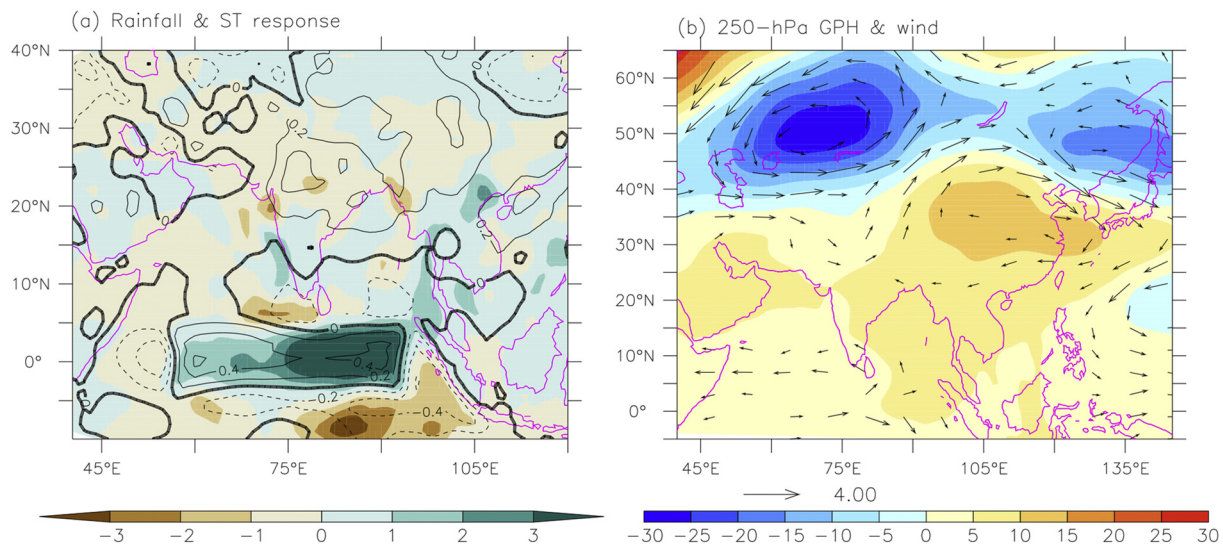


**Fig. 6.** Model experiment (a) surface temperature ( $^{\circ}\text{C}$ , black contours), rainfall (mm/day, color shade), and, (b) 250-hPa wind (m/s, black arrows) and GPH (m, color shade) response. (For interpretation of the references to color in this figure legend, the reader is referred to the web version of this article.)

prediction of the summer monsoon rainfall.

#### Data availability

The IMD gridded data is obtained by writing email to [ncc@im-d.gov.in](mailto:ncc@im-d.gov.in) and the reanalysis datasets are downloaded from their respective websites. The model data used in this study are available from the contributing author MKR on request.

#### Acknowledgments

Comments of anonymous reviewers dramatically improved the manuscript. Computational and graphical analyses required for this study have been completed with the free software xmgrace, NCL and Ferret.

#### References

- Abish, B., Cherchi, A., Ratna, S.B., 2018. ENSO and the recent warming of the Indian Ocean. *Int. J. Climatol.* 38, 203–214.
- Annamalai, H., Hafner, J., Sooraj, K.P., Pillai, P., 2013. Global warming shifts the monsoon circulation. *Drying South Asia. J. Clim.* 26, 2701–2718.
- Ashok, K., Guan, Z., Saji, N.H., Yamagata, T., 2004. Individual and combined influences of ENSO and the Indian Ocean dipole on the Indian summer monsoon. *J. Clim.* 17 (16), 3141–3155.
- Crétat, J., Terray, P., Masson, S., Sooraj, K.P., Roxy, M.K., 2017. Indian Ocean and Indian summer monsoon: relationships without ENSO in ocean–atmosphere coupled simulations. *Clim. Dyn.* 49 (4), 1429–1448.
- Dee, D.P., Uppala, S.M., Simmons, A.J., Berrisford, P., Poli, P., Kobayashi, S., Andrae, U., Balmaseda, M.A., Balsamo, G., Bauer, P., Bechtold, P., Beljaars, A.C.M., van de Berg, L., Bidlot, J., Bormann, N., Delsol, C., Dragani, R., Fuentes, M., Geer, A.J., Haimberger, L., Healy, S.B., Hersbach, H., Hólm, E.V., Isaksen, I., Kållberg, P., Köhler, M., Matricardi, M., McNally, A.P., Monge-Sanz, B.M., Morcrette, J.-J., Park, B.-K., Peubey, C., de Rosnay, P., Tavolato, C., Thépaut, J.-N., Vitart, F., 2011. The ERA-Interim reanalysis: configuration and performance of the data assimilation system. *Q. J. R. Meteorol. Soc.* 137, 553–597. <https://doi.org/10.1002/qj.828>.
- Gill, A.E., 1980. Some simple solutions for heat-induced tropical circulation. *Quart. J. Roy. Meteor. Soc.* 106, 447–462.
- Goswami, B.N., Madhusoodanan, M.S., Neema, C.P., Sengupta, D., 2006. A physical mechanism for North Atlantic SST influence on the Indian summer monsoon. *Geophys. Res. Lett.* 33 (2).
- Hendon, H.H., Wheeler, M.C., 2008. Some space-time spectral analyses of tropical convection and planetary-scale waves. *J. Atmos. Sci.* 65, 2936–2948. <https://doi.org/10.1175/2008JAS2675.1>.
- Huang, P., Huang, R., 2011. Climatology and interannual variability of convectively coupled equatorial waves activity. *J. Clim.* 24, 4451–4465.
- Jin, Q., Wang, C., 2017. A revival of Indian summer monsoon rainfall since 2002. *Nat. Clim. Chang.* 7, 587–595. <https://doi.org/10.1038/NCLIMATE3348>.
- Kinter, J.L.I.I., Fennessy, M.J., Krishnamurthy, V., Marx, L., 2004. An evaluation of the apparent interdecadal shift in the tropical divergent circulation in the NCEP-NCAR Reanalysis. *J. Clim.* 17, 349–361.
- Krishnamurti, T.N., Ardanuy, P., 1980. The 10–20 day westward propagating mode and breaks in monsoon. *Tellus* 32, 15–26.
- Krishnan, R., Sabin, T.P., Vellore, R., Mujumdar, M., Sanjay, J., Goswami, B.N., Terray, P., 2016. Deciphering the desiccation trend of the South Asian monsoon hydroclimate in a warming world. *Clim. Dyn.* 47 (3–4), 1007–1027.
- Kucharski, F., Bracco, A., Yoo, J., Molteni, F., 2008. Atlantic forced component of the Indian monsoon interannual variability. *Geophys. Res. Lett.* 35, L04706. <https://doi.org/10.1029/2007GL033037>.
- Kumar, K.K., Rajagopalan, B., Cane, M.A., 1999. On the weakening relationship between the Indian monsoon and ENSO. *Science* 284 (5423), 2156–2159.
- Lau, K.-M., Wu, H.-T., Bony, S., 1997. The role of large-scale atmospheric circulation in the relationship between tropical convection and sea surface temperature. *J. Clim.* 10, 381–392.
- Liebmann, B., Smith, C.A., 1996. Description of a complete (interpolated) outgoing longwave radiation dataset. *Bull. Am. Meteorol. Soc.* 77, 1275–1277.
- Matsumoto, T., 1966. Quasi-geostrophic motions in the equatorial area. *J. Meteor. Soc. Japan* 44, 25–43.
- Pai, D.S., Sridhar, L., Badwaik, M.R., Rajeevan, M., 2014. Analysis of the daily rainfall events over India using a new long period (1901–2010) high resolution ( $0.25^{\circ} \times 0.25^{\circ}$ ) gridded rainfall dataset. *Clim. Dyn.* <https://doi.org/10.1007/s00382-014-2307-1>.
- Paul, S., Ghosh, S., Oglesby, R., Pathak, A., Chandrasekharan, A., Ramsankaran, R.A.A.J., 2016. Weakening of Indian summer monsoon rainfall due to changes in land use land cover. *Sci. Rep.* 6, 32177.
- Qu, X., Huang, G., 2012. An Enhanced Influence of Tropical Indian Ocean on the South Asia High after the Late 1970s. *J. Clim.* 25, 6930–6941. <https://doi.org/10.1175/JCLI-D-11-00696.1>.
- Ramamurthy, K., 1969. Monsoons of India, some aspects of the ‘Break in the Indian southwest monsoon during July and August’. In: *Forecasting Manual No. IV-18.3. India Meteorological Department, Pune*, pp. 1–57.
- Raman, C.R.V., Rao, Y.P., 1981. Blocking highs over Asia and monsoon droughts over India. *Nature* 289, 271–273.
- Ramanathan, V., et al., 2005. Atmospheric brown clouds: Impacts on South Asian climate and hydrological cycle. *Proc. Natl. Acad. Sci. USA* 102, 5326–5333.
- Ramaswamy, C., 1956. On the sub-tropical jet stream and its role in the development of large scale convection. *Tellus* 8, 26–60.
- Ramaswamy, C., 1962. Breaks in the Indian summer monsoon as a phenomenon of interaction between the easterly and the subtropical westerly jet streams. *Tellus* 14, 337–349.
- Ratna, S.B., Cherchi, A., Joseph, P.V., Behera, S.K., Abish, B., Masina, S., 2016. Moisture variability over the Indo-Pacific region and its influence on the Indian summer monsoon rainfall. *Clim. Dyn.* 46, 949–965.
- Roxy, M.K., 2017. Land warming revives monsoon. *Nat. Clim. Chang.* 7 (8), 549.
- Roxy, M., Tanimoto, Y., Preethi, B., Pascal, T., Krishnan, R., 2013. Intraseasonal SST-precipitation relationship and its spatial variability over the tropical summer monsoon region. *Clim. Dyn.* 41, 45–61.
- Roxy, M.K., Ritika, K., Terray, P., Masson, S., 2014. The curious case of Indian Ocean warming. *Journal of Climate* 27 (22), 8501–8509.
- Roxy, M., Ritika, Kapoor, Terray, Pascal, Murtugudde, Raghu, Ashok, Karumuri, Goswami, B.N., 2015. Drying of Indian subcontinent by rapid Indian Ocean warming and a weakening land-sea thermal gradient. *Nat. Commun.* 6, 7423. <https://doi.org/10.1038/ncomms8423>.
- Saha, S., et al., 2013. The NCEP climate forecast system version 2. *J. Clim.* 27, 2185–2208.
- Saji, N.H., Goswami, B.N., Vinayachandran, P.N., Yamagata, T., 1999. A dipole mode in the tropical Indian Ocean. *Nature* 401, 360–363.

- Trenberth, K.E., Koike, T., Onogi, K., 2008. Progress and prospects for reanalysis for weather and climate. *Eos. Trans. Am. Geophys. Union* 89, 234–235.
- Vellore, R.K., Krishnan, R., Pendharkar, J., Choudhary, A.D., Sabin, T.P., 2014. On the anomalous precipitation enhancement over the Himalayan foothills during monsoon breaks. *Clim. Dyn.* 43, 2009–2031. <https://doi.org/10.1007/s00382-013-2024-1>.
- Vishnu, S., Francis, P.A., Shenoi, S.S.C., Ramakrishna, S.S.V.S., 2016. On the decreasing trend of the number of monsoon depressions in the Bay of Bengal. *Environ. Res. Lett.* 11 (1), 014011.
- Webster, P.J., Moore, A.M., Loschnigg, J.P., Leben, R.R., 1999. Coupled ocean-atmosphere dynamics in the Indian Ocean during 1997–98. *Nature* 401, 356–360.
- Yadav, R.K., 2009a. Changes in the large-scale features associated with the Indian summer monsoon in the recent decades. *Int. J. Climatol.* 29, 117–133. <https://doi.org/10.1002/joc.1698>.
- Yadav, R.K., 2009b. Role of equatorial central Pacific and northwest of North Atlantic 2-metre surface temperatures in modulating Indian summer monsoon variability. *Clim. Dyn.* 32, 549–563. <https://doi.org/10.1007/s00382-008-0410-x>.
- Yadav, R.K., 2016. On the relationship between Iran surface temperature and north-west India summer monsoon rainfall. *Int. J. Climatol.* 36, 4425–4438. <https://doi.org/10.1002/joc.4648>.
- Yadav, R.K., 2017a. On the relationship between east equatorial Atlantic SST and ISM through Eurasian wave. *Clim. Dyn.* 48, 281–295. <https://doi.org/10.1007/s00382-016-3074-y>.
- Yadav, R.K., 2017b. Mid-latitude Rossby wave modulation of the Indian summer monsoon. *Q. J. Roy. Meteor. Soc.* 2017. <https://doi.org/10.1002/qj.3083>. Published Online.
- Yadav, R.K., Srinivas, G., Chowdary, J.S., 2018. Atlantic Niño modulation of the Indian summer monsoon through Asian jet; *npj. Clim. Atmos. Sci.* 1, 23. <https://doi.org/10.1038/s41612-018-0029-5>.